Comparison of low-frequency data from co-located receivers

Kevin W. Hall, Gary F. Margrave and Malcolm B. Bertram, CREWES, University of Calgary*

Summary

A low-frequency sensor comparison survey was acquired at the University of Calgary's test site near Priddis Alberta in August 2009. Portable calibrated broadband seismometers, analog 3C 10 Hz geophones and two makes of digital 3C accelerometers were deployed at 1 m receiver line spacing, and used to record weight-drop and EnviroVibe (this report) sources at two source points located 50 m from the end of the receiver lines. This study shows that least-squares-subtraction scalars (LSSS) depend on amplitude, frequency, phase, source-receiver offset, quality of sensor placement in or on the ground. LSSS show good promise for future use in quantitative sensor comparison studies.

Introduction

In August 2009 the University of Calgary had access to eight Nanometrics Trillium 240 seismometers which were destined to be deployed to temporary sites around Alberta as part of a monitoring project. While these units were still in Calgary, it was decided to attempt to compare the low frequency response of 10 Hz geophones to these calibrated seismometers. As an additional experiment, with the co-operation of ION and CGGVeritas, ION Vectorseis and Sercel DSU3 accelerometers were also deployed at the University of Calgary's Priddis test site. The ION spread used Vectorseis units recorded on a Scorpion system, and the Sercel spread used DSU3 sensors recorded on a Sercel 428XL system.

The 10 Hz geophone spread was laid out as 80 geophones at 1m spacing to provide more detail of surface motion (Figure 1). Trillium, Vectorseis and DSU3 sensors were set up alongside the geophones at 10 m receiver spacing. Holes were augured for the nail-type geophone/MEMS cases. Shallow holes were dug deep enough to remove top-soil (~20 cm) and cement patio blocks were placed and coarsely leveled in the holes for the seismometers. Seismometers and 3C geophones were oriented inline; accelerometers were aligned to magnetic north.

The sources for this survey were an accelerated weight drop unit fired with and without elastic tensioning bands and the University of Calgary's IVI EnviroVibe at 50 m offsets to the north and south of the receiver lines (Figure 1). With the focus on low frequency, the EnviroVibe was operated well outside its design specifications, and many phase errors were observed in the field for frequencies below ~8 Hz. Sweeps acquired were: 3 Hz and 5 Hz (at 3% and 5% of maximum power) mono-frequency sweeps, and a suite of 2-10 Hz and 2-100 Hz linear sweeps (at 10% of maximum power) with 10, 30 and 50 s sweep lengths. All EnviroVibe data were recorded uncorrelated. Long tapers were used at the low-frequency end of the sweep to prevent damaging the EnviroVibe.

For this initial study, we focused on vertical component data from the uncorrelated 2-10 Hz sweeps. We wish to determine if frequency dependent least-squares-subtraction scalars (LSSS) can provide useful information in regards to sensor comparisons.

Method

The amplitudes of any two data traces (S_1 and S_2), can be matched by multiplying one of the traces by some constant, a. The best-fit constant a can be determined in a least-squares-subtraction sense by defining some number

$$\varepsilon = \sum_k (S_{1k} - aS_{2k})^2, \qquad (1)$$

where k represents individual samples within each data trace. Differentiating ε with respect to a and requiring that the result equals zero gives

$$\frac{1}{2}\frac{\partial \varepsilon}{\partial a} = \sum_k S_{1k}S_{2k} - a\sum_k S_{2k}^2 = 0. \qquad (2)$$

Equation (2) can then be solved for a:

$$a = \frac{\sum_k S_{1k}S_{2k}}{\sum_k S_{2k}^2}, \qquad (3)$$

where equation (3) is equivalent to the zero-lag cross-correlation divided by the zero-lag auto-correlation.

If trace S_1 is a copy of trace S_2 with amplitudes scaled by a constant b, the LSS scalar a will be equal to b for all frequencies. If S_1 is an exact copy of S_2 (b = 1), a should equal 1, but, if S_2 is progressively time-shifted relative to S_1, the LSS scalar varied between -1 and +1 for a synthetic mono-frequency sweep, and between -0.8 and +1 for a synthetic 2-10 Hz sweep (not shown).

In order to investigate amplitude dependence on frequency, data traces were bandpass filtered before calculating the LSSS with a series of 1 Hz wide bandpass filter windows from 2-10 Hz in 0.1 Hz increments. This means that data points plotted at 4 Hz in subsequent figures are the results from equation (3) for two input traces filtered with a 3.5-4.5 Hz pass-band.

Comparison of low-frequency data from co-located receivers

Data preparation

We were unable to use the raw uncorrelated data as originally intended for three main reasons: 1) while three of the recording systems sampled the wavefield at a 2 ms sample rate, the seismometer data were sampled at 10 ms, 2) seismometer data were continuously recorded (no trigger) and 3) the Sercel/DSU3 system was manually triggered for each shot (no time-break).

Source gathers were extracted from the seismometer data using the time of shot recorded in the Aries observer's notes. The data were coarsely aligned to a time zero that was arbitrarily set to 100 ms. The seismometer gathers were then de-biased and re-sampled to a 2 ms sample rate to match the other datasets. De-biasing was required since low frequency components (less than 1 Hz) in the seismometer data were truncated when the gathers were extracted, resulting in an apparent DC bias.

Accelerometer data were integrated to obtain velocity curves. The geophone and accelerometer data were bandpass filtered (2-10 Hz) to attenuate higher frequency source, generator and power-line noise, then aligned to the seismometer traces by calculating maximum positive cross-correlations and sub-sample shifting the traces (Figure 2).

The data compare well visually, but minor differences can be seen throughout the sweep and the seismometer response is noticeably different at the end of the sweep (larger amplitudes, right side; Figure 2).

Results

Figure 3 shows receiver gathers of the LSSS calculated for all 2-10 Hz sweeps at the northern source point. Subtle differences are present in the LSSS for the different length sweeps. Dashed lines in Figure 3 have the same slope, and highlight a source-receiver offset dependence of the LSSS. Data from the southern SP exhibit an opposite slope (not shown). Black rectangles highlight a LSSS anomaly 90 m from the northern SP. This anomaly can be clearly seen on the geophone and Vectorseis comparisons, but is not clearly seen on the DSU3 plot.

Figure 4 shows the averaged LSSS curves for all 2-10 Hz sweeps (both source points). This is essentially a sideways view of the averaged results shown in Figure 3

Discussion

The least-squares-subtraction scalar has been shown to depend on amplitude and phase in synthetic data. Real data results show that the LSSS is frequency dependent (Figures 3 and 4). The results for station 5 (90 m south of the north source point) of the real data show that it also depends on the quality of sensor placement in or on the ground (black rectangles; Figure 3). The LSSS anomaly at station 5 can be clearly seen on the geophone, integrated Vectorseis and integrated DSU3 LSSS curves, implying that the seismometer placement at station 5 was somehow different than at adjacent stations. Finally, the dashed lines in Figure 3 highlight source-receiver offset dependent effects in the LSSS.

The geophone data amplitudes are 10^7 times smaller than the seismometer amplitudes, and the Vectorseis data are similar, at 10^9 times smaller. The raw DSU3 amplitudes are closest to the raw seismometer amplitudes. If instrument response was identical or merely scaled in amplitude, the LSSS curves should be horizontal lines. The fact that they are not may be explained by the observation that filtering with a 2-10 Hz pass-band before aligning the traces gives a different LSSS result than filtering with a 2-40 Hz pass-band, or not filtering at all. This suggests that we may need to examine trace alignment after applying the narrow-pass filters, and possibly consider doing the trace alignment after the filter. Performing the calculations in this manner would take considerably more computation time.

The geophone versus seismometer LSSS curve looks quite different than the accelerometer versus seismometer curves. The general decrease in geophone amplitude towards lower frequencies relative to the seismometer data (increase in LSSS curve; Figure 4) is likely due to our narrow-pass filters starting to see the low-cut filter in the Aries recording system.

The Vectorseis and DSU3 versus seismometer LSSS curves are quite similar to each other, disregarding scale. These data appear to match the seismometer data best below 4 Hertz, and less well at higher frequencies. Again, this result could be due to issues with trace alignment after narrow-pass filtering.

The fact that the Vectorseis and DSU3 LSSS curves are similar to each other, but different to the geophone result shows that the LSSS could be used to conduct sensor comparisons.

Acknowledgements

We would like to thank the field crew, which included University of Calgary (CREWES) faculty, staff and students, as well as Kris Dash from ARAM Systems, Tom Preusser and Aaron Kennedy from CGGVeritas, Brett Frederickson from ION, and Waled Bin Merdhah from ERCB/Alberta Geological Survey. We would also like to thank Dr. David Eaton for allowing us to use the seismometers for this experiment.

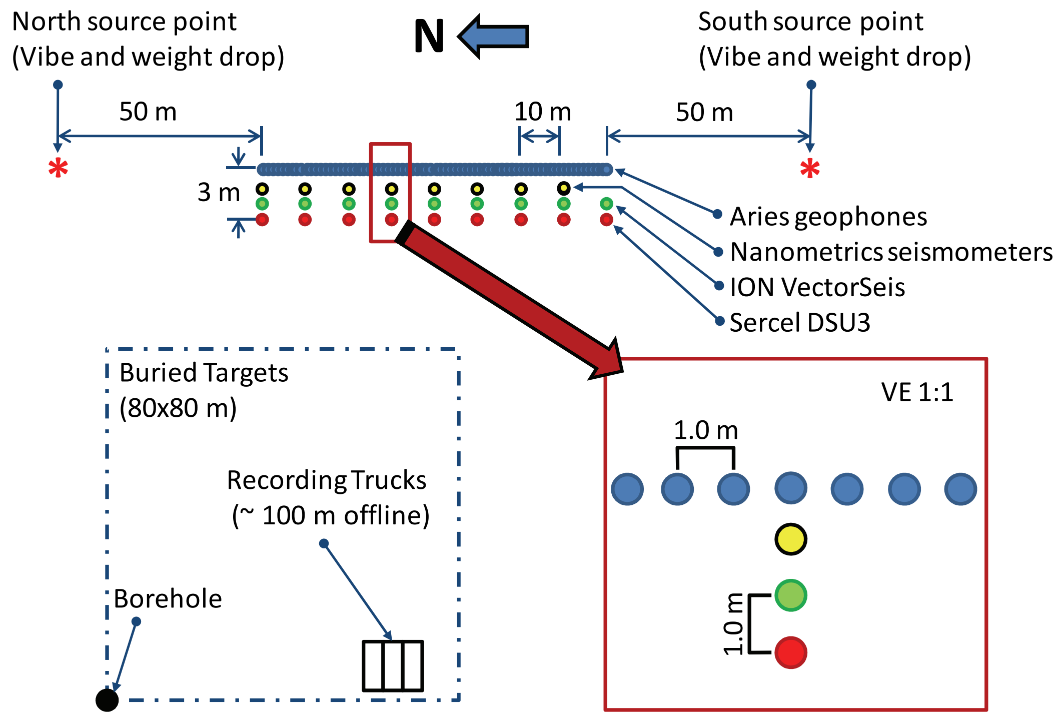

Figure 1: Schematic of survey layout at the University of Calgary's Priddis test site.

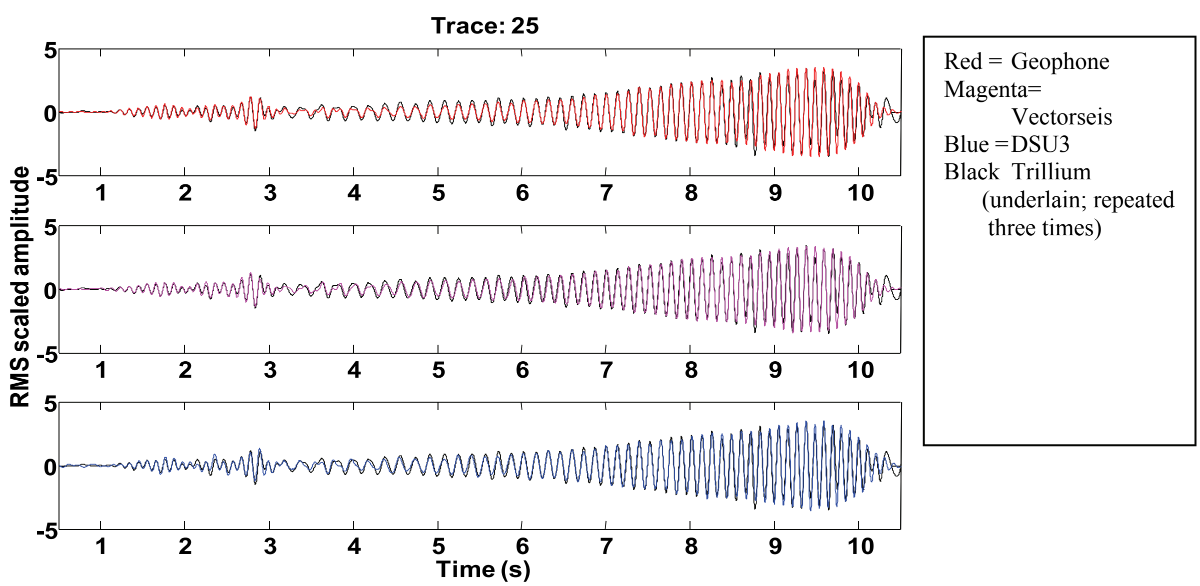

Figure 2: Vertical component uncorrelated traces from 50 m south of the north SP for a 10 s 2-10 Hz sweep.

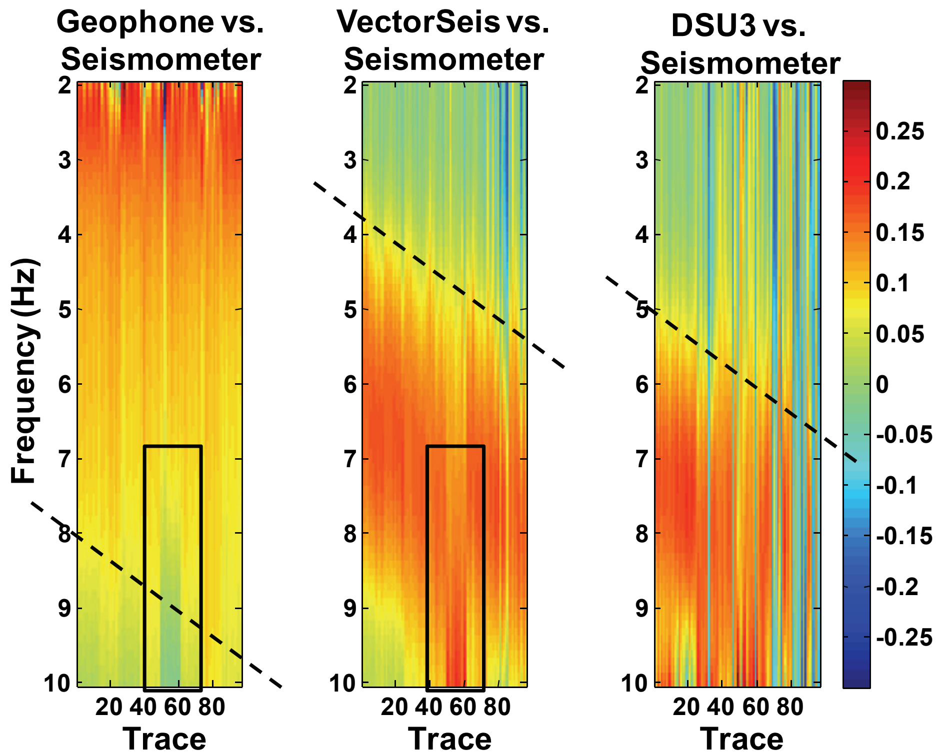

Figure 3: Receiver gathers of least-squares-subtraction scalars (LSSS) for all 2-10 Hz sweeps acquired at the north SP, normalized for display.

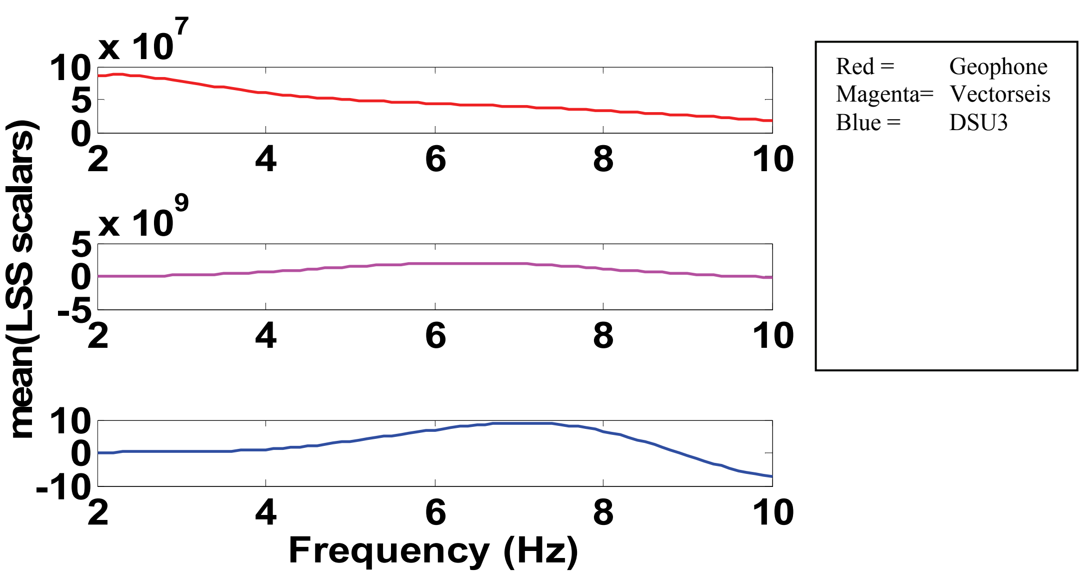

Figure 4: Averaged LSSS for all sensors and for all 2-10 Hz sweeps.